

Tec Nano 2019

# Pyrolytic Carbon from Novolac Epoxy Resin Compressed before Photocrosslinking and Pyrolysis

Saeed Beigi-Boroujeni<sup>1</sup>, Osamu Katagiri-Tanaka<sup>1</sup>, Braulio Cardenas-Benitez<sup>1</sup>, Sergio O. Martinez-Chapa<sup>1</sup>, Alan Aguirre-Soto<sup>1,\*</sup>

<sup>1</sup>Tecnologico de Monterrey, School of Engineering and Sciences, Av. Eugenio Garza Sada Sur, Monterrey, 2501, N.L., Mexico.

## Abstract

The so-called SU-8 formulation, originally designed as a negative photoresist, has become the gold standard for the fabrication of microelectromechanical systems (MEMS) due to its relatively versatile processability and to the unique set of properties of the carbon obtained from pyrolysis of the patternable Bis-Phenol A Novolac Epoxy (BPNE) oligomer contained therein. Here, we investigate the possibility of increasing the degree of graphitization and electrical conductivity of BPNE-derived carbon by mechanically compressing the uncured oligomer pre-pyrolysis. BPNE sheets were casted, compressed and photocrosslinked to “freeze” the material in a strained configuration before carbonization. The electrical sheet resistance was determined using the four-point probe technique. The relative  $sp^2/sp^3$  content and the degree of crystallinity were compared by Raman and XRD spectroscopy. It was hypothesized that applying compressive loads of up to 2000 kg at 90°C would suffice to increase the crystallite size and the mesoscale order of the percolated graphenic carbon network by promoting the alignment of the aromatic segments from the phenolic groups before pyrolysis. However, negligible variations in the resistivity and  $sp^2$ -carbon microstructural features were observed when compressing millimetric sheets of BPNE as compared to uncompressed samples, suggesting that higher forces and temperatures may be required to synthesize BPNE-derived glass-like carbon materials with a slightly more graphitic character.

[copyright information to be updated in production process]

**Keywords:** SU-8 photoresist; Epoxy resin; Cationic photopolymerization; Stress-induced graphitization; Pyrolysis; Carbon materials.

## 1. Introduction

Carbon materials are uniquely interesting in that from a seemingly simple paradigm, heating organic matter, a broad range of complex structures emerge, each displaying a unique set of properties. It is an epitome of how complexity and diversity arise in Nature from a single building unit with a relatively small set of rules involved in its transformation. Precisely this phenomenon is what has gained the attention of many trying to find the “ultimate” material, while, somewhat ironically, makes it remarkably difficult to controllably yield a carbon material with a desired set of properties. Carbon materials exhibit complexity as a collection of degrees of freedom at multiple scales varying through a multidimensional continuum, where the precise values of each one of them contributes to the unique set of properties that characterize the material. Some of the most important features from the molecular to the mesoscale are hybridization, crystallite size, percolation, anisotropy, impurities/imperfections, and porosity. The combination of these intertwined multiscale features leads to the broad spectrum of macroscopic characteristics that constitute the profile or “fingerprint” of the carbon material. For instance, carbon materials with a range of chemical inertness, electrical conductivity, mechanical strength, optical transparency, and electrochemical stability have been

\* Corresponding author. Tel.: +52 1 81 11706549.

E-mail address: [alan.aguirre@tec.mx](mailto:alan.aguirre@tec.mx)

synthesized and employed for various purposes [1–8]. This article focuses its discussion on materials found in between two of the various possible categories, namely the so-called glass-like and graphite-like families of carbon materials, often grouped in the pyrolytic carbons class. Here, we jump between both classes of carbon materials as we investigate the possibility of altering the profile of a typical glass-like material by giving it a slightly more graphitic character.

The chemical inertness, electrical conductivity and electrochemical properties of some pyrolytic carbon materials have made them popular as potential candidates to replace silicon in components for microelectromechanical systems (MEMS): sensors, batteries, capacitors, and transistors [9–11]. Glass-like carbon materials, specifically, are attractive from a practical point of view given their characteristic combination of electrochemical stability, redox potentials, thermal resistance, electrical conductivity and biocompatibility, as well as their relatively low-cost fabrication methods. Therefore, a substantial amount of research has been dedicated to the investigation of cost-effective methods to fine-tune the properties of glass-like carbon materials, to extend the library of glass-like carbon precursors, and to expand the applications of these materials. Our long-term goal is to synthesize carbon materials with a set of properties suitable for photo- and photoelectro-chemical catalysis, where one of the most important characteristics is the resistance to strongly oxidizing or reducing environments, while retaining competitive electron transfer rates.

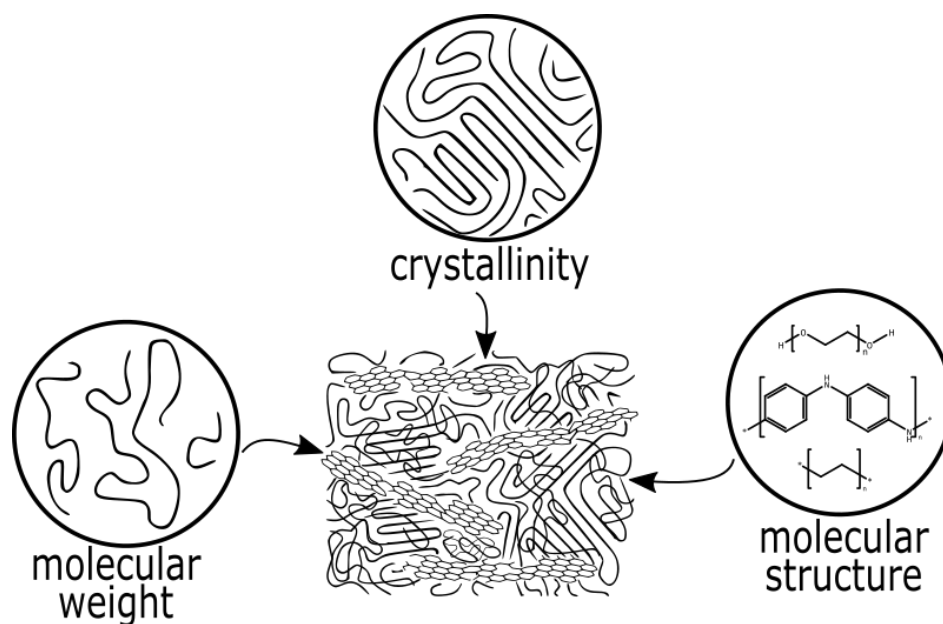


Figure 1. Molecular to mesoscale structural features of synthetic polymers influence the emergence of specific microstructural features in polymer-derived carbon materials after pyrolysis.

Carbon materials with glass-like features have been derived from synthetic organic polymers by appropriately tuning the pyrolysis protocol as a function of the molecular structure of the carbon source (Figure 1) [12–14]. As a result, the pyrolysis of polymers has been widely studied with the hope of producing materials with molecular to mesoscale features that yield desired combinations of properties, e.g. unique combination of carbon allotrope content, crystallite size, and porosity to obtain a low density chemically-inert material. A myriad of polymer precursors has been tested since the seminal crystallinity studies of the 20th Century by Rosalind Franklin. Since then, many temperatures and atmospheres, or lack thereof, have been analyzed in terms of their impact on the final microstructure of the carbon material [12–18]. From there, it is generally agreed upon that the molecular structure of the polymer appears to be the most important factor in determining the profile of the final carbon material. However, the importance of other variables was highlighted in these studies, such as the crosslink density, sample dimensions, thermal treatment curve and type of pretreatment. The latter refers to any additional processing steps performed before pyrolysis to alter the mesoscale structure of the polymer to be carbonized. It is important to note that the profile of properties of the final carbon material must justify the pyrolysis of the often-expensive synthetic polymers, which

typically have outstanding properties of their own. For instance, most synthetic organic polymers have either insufficient redox potentials or chemical resistance to be used as photocatalysts, while their derivative carbon materials may display more suitable properties for the purpose.

It has been known for some time that phenol-formaldehyde resins are excellent candidates for the fabrication of glass-like carbon. Specifically, the so-called SU-8 formulation has turned into one of the most popular precursors for the fabrication of electrically conductive glass-like carbon materials with outstanding aspect ratios [12-13]. Yet, the precise mechanism behind why and how this particular formulation can form carbon materials with such a unique set of properties remains incomplete. The SU-8 formulation remains bound to a certain degree of industrial secrecy, which complicates its analysis. From what can be discerned from the available information, it contains an oligomer called Bis-phenol A Novolac Epoxy (BPNE) and based on a number ( $n$ ) of bisphenol units with  $(2n)$  pendant epoxide groups susceptible to cationic polymerization. The number of repeating units is eight in the standard commercial formulations, but the polydispersity is not reported. The chain growth polymerization of this prepolymer is typically initiated by an acid generator activated by either thermal or electromagnetic energy, and results in the formation of a crosslinked material by ring-opening the epoxide groups. The most popular photoinitiator (PI), photoacid generator, for these formulations seems to be a sulfonium salt, e.g. triarylsulfonium hexafluoroantimonate salt. The aforementioned PI produces both free radicals and cations upon photolysis under UV radiation. Cyclopentanone is utilized as high-volatility solvent enabling the casting of the oligomer/PI/salts mixture (Figure 2) [12–14]. This solvent is required to adjust the viscosity to facilitate the casting, spin coating or electrospinning of the solid-state oligomer, and is mostly evaporated before pyrolysis. Therefore, we will refer to our carbon source material as simply Bis-phenol A Novolac Epoxy (BPNE), considering that the other left-over molecules from the formulation, PI and salt additives, are present in relatively such low quantities that their contribution towards the properties of the pyrolytic carbon material is small.

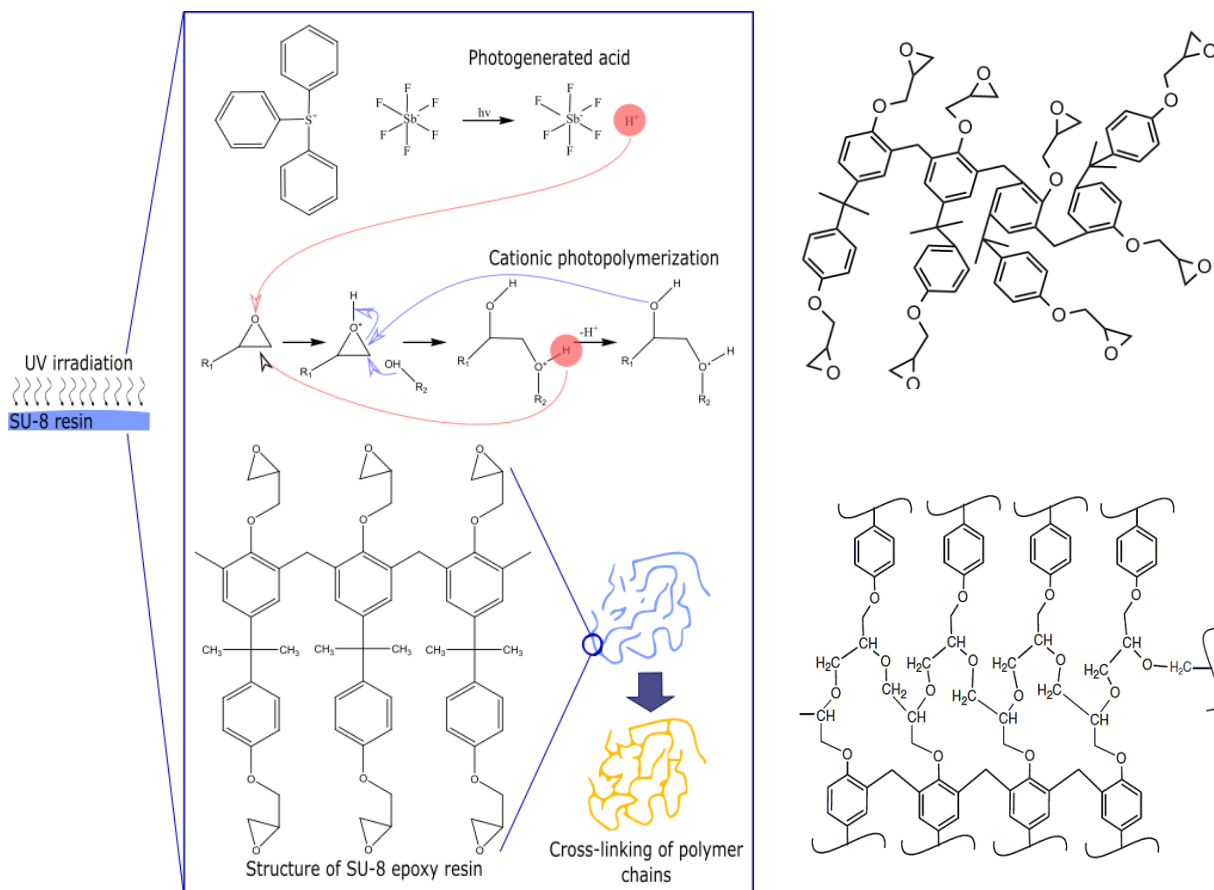


Figure 2. Photocrosslinking of Bis-phenol A Novolac Epoxy upon exposure to 365 nm light in the presence of sulfonium salt showing the structures of the glycidyl ether based prepolymer before and after the cationic chain-growth polymerization on the right.

While polymers, such as crosslinked BPNE, yield glass-like carbon, some of the latest efforts have centered around the possibility of giving them slightly more graphitic characteristics by modifying the standard MEMS fabrication method. Cardenas-Benitez and coworkers proposed that internal mechanical forces related to the pyrolysis-induced shrinkage of photocrosslinked BPNE microwires suspended between BPNE posts are responsible for the substantial shrinkage, deformation and buckling of suspended fibers [12]. The study showed that the structures shrank up to 70% of their pre-pyrolysis size, which is typical in the formation of glass-like carbon. Canton et al. [14] deposited BPNE fibers over BPNE posts to form monolithic microstructures, where the shrinkage and elongation of the suspended microfibers during pyrolysis appears to have influenced the final electrical properties. As the posts shrink during pyrolysis, the shrinkage-induced internal forces seem to result in the buckling of the suspended fibers. Evidence appears to suggest that the electrical conductivity increases when fibers are elongated and stretched as the diameter decreases during free-volume loss [14]. These observations were the seed of our hypothesis that one could increase the graphitization in BPNE-derived carbon materials by straining the uncured BPNE just before crosslinking the multifunctional epoxide into the thermosetting polymer network to be pyrolyzed. However, it can be reasonably expected that proving this hypothesis on the suspended microwires fabricated by Cardenas-Benitez and coworkers will be a remarkable experimental challenge considering the geometry and the precision required to controllably stress the precursor material at such scales. This led us to propose the present proof-of-concept investigation of the possibility of altering the electrical conductivity of carbon materials derived from BPNE in the form of millimetric sheets instead of microstructures, as these can be more easily compressed and manipulated before photocrosslinking and pyrolysis.

A few chemical and physical methods have been reported for the production of glass-like carbon with more graphitic characteristics by purposely altering the mesoscale morphology of macroscopic polymer samples before pyrolysis [14–17]. Specifically, the idea of mechanically compressing polymers to increase the crystallinity before carbonization, and produce a carbon material with a higher electrical conductivity, was successfully employed by Ghazinejad and coworkers [17]. In that case, the effect of compression and tension on the degree of graphitization and molecular alignment of mats of polyacrylonitrile (PAN) fibers was investigated. The forces involved in far-field electrospinning using carbon nanotubes as templating agents contributed to the increase in the orientation of the macromolecular chains before pyrolysis. Thermal crosslinking via cyclization of the nitrile groups was employed to lock the polymer into a more crystalline network promoted by the mechanical stresses. Mats of crosslinked PAN fibers were pyrolyzed for samples with and without the mechanical strain. Their results showed that by combining thermal crosslinking and mechanical stress, the previously “non-graphitizable” PAN produced a more graphitic carbon material as evidenced by the Raman spectral features and electrical conductivity. The potential contribution of a reduction in the macroporosity of the samples towards the increase in electrical conductivity was not discussed. Compression appears to have resulted in carbon materials with higher conductivity than samples that were crosslinked under tension. These findings support our hypothesis that the electrical conductivity of polymer-derived carbon materials may be increased when mechanically pretreating macroscopic samples. It is important to point out that the idea herein is to compress casted solid sheets of the uncured resin close the melting point, as opposed to the previously used macroporous mats of polymer fibers at higher thermal crosslinking temperatures (Figure 3). Compression of the uncured Novolac resin at a temperature around the melting point ( $T_m$ ) may be expected to be sufficient to increase the crystallinity of the macromolecular network to be carbonized. The latter given the possibility of mechanically inducing the formation of more crystalline domains in the polymer through the alignment of the bis-phenolic groups via  $\pi$ - $\pi$  stacking. It is worth noting, that applying the mechanical stress on the crosslinked BPNE instead of uncured resin was expected to have a lower effect on the crystallinity, considering the  $T_g$  ( $> 200$  °C) of UV-crosslinked BPNE resin.

Additional insights supporting our hypothesis were reported as variations in electrical conductivity of carbon electrodes upon the application of mechanical stresses, and proposed to be due to an increase in the alignment of the polymer linear segments within the fibers, i.e. in a similar fashion as in the templating phenomenon that occurs in the electrospinning of synthetic polymers aided by carbon nanotubes and graphene sheets [18,19]. The electrical conductivity of carbon electrodes increased after pyrolysis, as the precursor macromolecular chains align within the fibers yielding carbon structures with higher crystallinity as a result of the internal mechanical stresses that develop during pyrolysis. The use of carbon nanotubes in combination with the hydro-electromechanical forces from the electrospinning process also appears to result in the alignment of polymer chains [16,17,20], leading to the production of carbon materials with superior electrical conductivity. These cases are great exemplars of the use of the templating mechanism to align polymer chains along the flow axis to make conductive materials from patternable polymers that have been proposed for several applications, including wearable devices and flexible electronics [21].

In this study, we searched for variations in the microstructure and the electrical resistivity of carbon materials produced from the pyrolysis of millimetric sheets of photocrosslinked BPNE that may arise from the use of mechanical compression as a pretreatment before photocrosslinking and pyrolysis. The aim of this article is to evaluate whether the mechanical compression pretreatment at close to melting temperature of BNPE samples is a viable method to produce glass-like carbon materials with slightly more graphitic characteristics without increasing the temperature during pyrolysis. From a practical point of view, the motivation is to match the fabrication conditions to the molecular structure of patternable polymer precursors in order to produce carbon materials that possess a desired combination of properties. The present study serves as a first attempt to demonstrate if such a relatively simple modification to the standard fabrication protocol can be reliably used to produce higher conductivity glass-like carbon. Furthermore, we intend this contribution to aid in the elucidation of structure/synthesis/properties relationships that serve as insights into the uniqueness of the SU-8 chemistry and that guide the fabrication of novel materials. Ultimately, we hope to expand the application portfolio of electrically insulating thermosetting photopolymers by developing methods to fabricate carbon materials with complex geometries having suitable properties for photo- and photoelectro-catalysis.

## 2. Materials and Methods

### 2.1. Casting, compressive pretreatment, photocrosslinking and pyrolysis of Bis-phenol A Novolac Epoxy sheets

The SU-8 2100 formulation was purchased from MicroChem Corp. (now Kayaku Advanced Materials, Westborough, MA, USA) containing the multifunctional oligomer bisphenol A Novolac epoxy and PI, and used as received according to the sheet casting protocol shown below. A soft-lithography kit, namely Sylgard 184 (Dow Corning, MI, USA), based on poly-dimethyl siloxane (PDMS) chemistry was purchased and used without any modification, according to the manufacturer instructions, to fabricate non-stick molds for the casting of BPNE sheets.

The standard MEMS fabrication protocol is diagrammatically represented in Figure 3 along with the compression pretreatment modification studied herein. The SU-8 formulation was casted into rectangular sheets with dimensions of 10-15 mm x 25-30 mm x 1-1.5 (or 0.6) mm using the PDMS molds mentioned above. The cyclopentanone was evaporated by increasing the temperature to 75 °C for 4h using a standard hot-plate to ensure most of the solvent is absent for the next steps. For the case of the mechanically pretreated samples, the pre-heated SU-8 sheets were compressed by quickly applying a constant load of up to 2000 kg for 30 minutes to yield a maximum compressive stress of around 50 MPa, which was kept constant over the sample for 30 minutes at 90°C. The thickness of the compressed samples decreased from 1-1.5 mm to 0.6 mm after compression. The compressed samples were immediately thereafter exposed to 365 nm light in a UV chamber (DYMAX 2000-EC equipped with a halogen bulb with an intensity of approximately 105 mW/cm<sup>2</sup>) for 60 seconds. Control samples were fabricated at a smaller initial thickness (0.6 mm) and exposed to UV light for 60 seconds before pyrolysis, but without having being compressed.

The last step was to pyrolyze both groups of photopolymerized samples with and without the compression step at 1000 °C under a continuous flow of ultra-high purity nitrogen (N<sub>2</sub>, 99.99%) atmosphere at about 5 L/min sustained during the entire heat-treatment step. The samples were pyrolyzed in a PEO 601 furnace (ATV Technologie GmbH, Vaterstetten, Germany) according to the following carbonization protocol: pre-carbonization— (1) the temperature was increased from room temperature to 300°C at a heating rate of 30°C/min, (2) temperature was kept at 300 °C for 3 hours, carbonization— (3) the temperature was ramped to 900°C at 10°C/min and kept for 1hour, and (4) the temperature was brought back to room temperature at 30°C/min. A standard annealing stage was not used in this study. This protocol was based on a previously reported fabrication protocol to produce MEMS from patterned photoresists such as SU-8 for electrochemical sensors, and expecting to obtain pyrolytic carbon material with optimal properties at these temperatures and heating rates. All samples had dimensions of 10-15 mm x 25-30 mm x 0.6 mm when entering the furnace. During pyrolysis, the thickness of all the samples decreased to approximately 0.5 mm. The samples that were going to be compressed were casted in molds with higher thickness (1.5 mm) so that after applying the compressive force the thickness went down to 0.6 mm and then to 0.5 mm after pyrolysis. Control samples, without compression pretreatment, were casted in smaller PDMS molds to yield the same final thickness after pyrolysis.

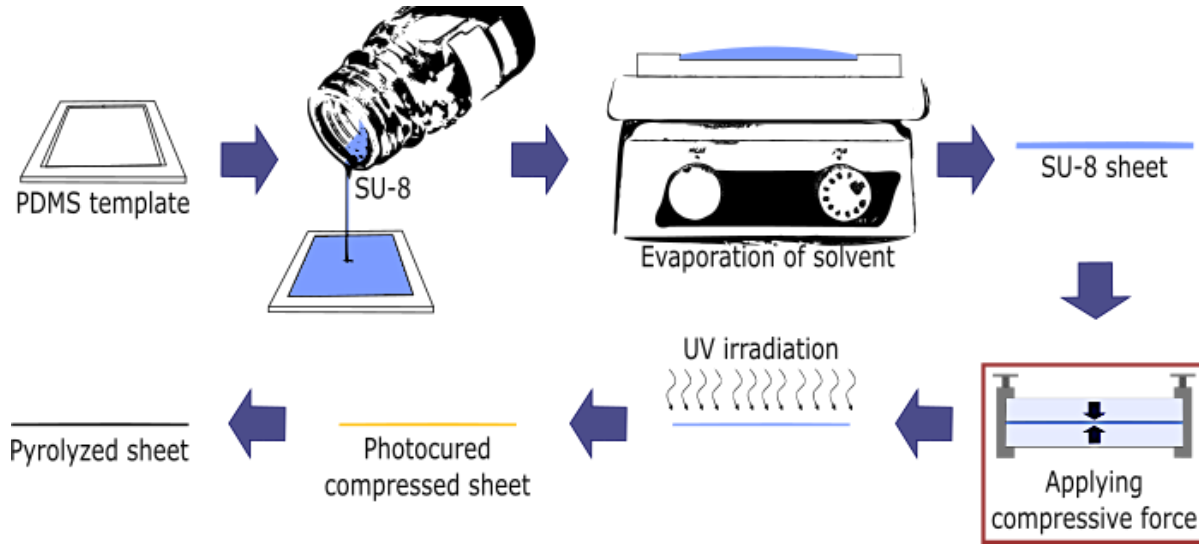


Figure 3. Procedure employed for the fabrication of carbon materials derived from SU-8 with addition of a mechanical pretreatment step where the uncured oligomer is isothermally compressed before photopolymerization and carbonization.

## 2.2. XRD and Raman spectroscopy

X-ray diffraction (XRD) patterns were obtained for all samples recording over a  $2\theta$  in the range of  $5-55^\circ$  using a Miniflex 600 spectrometer (Rigaku, Tokyo, JPN) equipped with the  $\text{CuK}\alpha$  radiation source.

Analysis of the relative  $\text{sp}^2$ -hybridized carbon content was carried out using an InVia Raman Microscope (Renishaw, Wotton-under-Edge, UK) equipped with a 532 nm laser. The Raman maps and the averaged Raman spectra were collected across  $25 \mu\text{m}^2$  tiles. Lorentzian fitting was used in MATLAB to deconvolute the bands of interest and analyze their maxima and areas.

## 2.3. Four-point probe measurements

The electrical sheet resistance ( $\Omega/\square$ ) of the samples was estimated using the four-point-probe method and then converted to bulk resistivity. Four electrical probes were placed in-line in contact with the top surface of square shaped samples of casted and uncured BPNE resin using a spacing of 5-10 mm between the needles. An electrical current, varied between 0 and 1.5 amperes, was applied through the sample from the outer two probes, while the voltage drop is measured by the inner probes [22]. For the dimensions and geometry of the samples used herein, the bulk resistivity was calculated using an equation (1) adapted from the four-point method to the geometry and size of our samples:

$$\rho = \frac{\pi * t}{\ln(2)} \left( \frac{V}{I} \right) \quad (1)$$

Where, V is the voltage, I is the applied current, and t is the thickness of the thin sample sheet.

## 3. Results and discussion

We began by searching for variations in the resistivity of the BPNE sheets at ambient conditions using the four-point probe technique in an in-line configuration for the 0.5 mm thick samples with and without the compression pretreatment. We observed a negligible difference in the resistivity values between the samples that were compressed before photocrosslinking and the samples that were photocrosslinked and pyrolyzed without mechanical compression. It was ensured that the all samples had approximately the same final thickness for both groups of samples. At least three samples were tested for every group. Our results suggest that there is no variation in the resistivity that correlates

with the use of compression before pyrolysis. We obtained the same value,  $18 \text{ m}\Omega \cdot \text{cm}$ , for the resistivity of pyrolyzed sheets both with (M-SU-8) and without (SU-8) the compression pretreatment (Table 1 and Figure 4). It is possible that the irregularities and roughness of the surface of the pyrolyzed sheets may have led to imprecisions in the four-point-probe measurements as the electrical contact with the surface of the sample could have been non-ideal. However, our values have a magnitude that fits well against previously reported values for commercial bulk-manufactured glassy carbon,  $1\text{-}5 \text{ m}\Omega \cdot \text{cm}$  (Table 1). Materials derived from the pyrolysis of BPNE samples of various geometries also have reported values in the same range. For instance, Pramanick et al. [23], reported that the resistivity of pyrolyzed SU-8 samples oscillated around  $37 \text{ m}\Omega \cdot \text{cm}$  once a temperature of 900 is reached in the pyrolysis protocol. Therefore, our measurements appear to give reasonable values despite the surface roughness of the pyrolyzed sheets obtained after the compression pretreatment, which could have affected the electrical contact with the sample. This method appears to be sufficient to be able to detect the variations we had originally hypothesized that would occur as a result of the mechanical compression pretreatment, order of magnitude variations. Therefore, these initial results suggest that the mechanical pretreatment may not be sufficient to alter the electrical properties in the BPNE samples used here.

**Table 1. Comparison of sheet resistivity, conductivity, and  $I_D/I_G$  ratios for several carbon materials.**

Carbon Material	Resistivity ( $\text{m}\Omega \cdot \text{cm}$ ) <sup>f</sup>	Conductivity (S/m)	$I_D/I_G$	Ref.
Pyrolyzed Pure PAN <sup>a</sup>	-	150-250	1.26	[17]
Pyrolyzed PAN-CNT <sup>b</sup>	-	450-600	1.00	[17]
Pyrolyzed M-PAN-CNT <sup>c</sup>	-	4,900-5,000	0.69	[17]
Glassy carbon	-	-	1.04	[12]
Pyrolyzed SU-8	36.9	2,705 <sup>g</sup>	-	[23]
Pyrolyzed iodinated PVA <sup>d</sup>	-	50-400	0.98	[24]
Pyrolyzed SU-8 sheet	9.3	10,752 <sup>g</sup>	1.02	[25]
Pyrolyzed M-SU-8 sheet <sup>e</sup>	18	5,555 <sup>g</sup>	1.02	Current work

<sup>a</sup> Polyacrylonitrile

<sup>b</sup> Carbon nanotubes infused PAN

<sup>c</sup> Mechanically treated PAN-CNT

<sup>d</sup> Poly (vinyl alcohol)

<sup>e</sup> Mechanically treated SU-8

<sup>f</sup> Pyrolyzed at 900 °C

<sup>g</sup> Calculated based on the bulk resistivity

From the resistivity values, we estimated a conductivity of around 5,555 S/m (Table 1), which appears to be a mid-range value for BPNE-derived carbon materials [12]. Overall, the value for the electrical conductivity obtained here lies closer to the values typically observed for amorphous carbon,  $1\text{-}2 \times 10^3 \text{ S/m}$ , than those for graphite,  $2\text{-}3 \times 10^5$ , with aligned basal planes. The electrical conductivity of glass-like carbon materials in general has been reported to reach values of  $2 \times 10^4 \text{ S/m}$  and higher if heat-treated appropriately and depending on the sample geometry and dimensions. For instance, higher electrical conductivities are typically achieved in polymer-derived carbon materials synthesized at higher pyrolysis temperatures and smaller dimensions, nano- and micro-scales as those used for MEMS. Interestingly, in the previous investigation of variations in the conductivity of carbon materials derived from millimetric samples of a mechanically-strained mat of PAN nanofibers, conductivity increased one order of magnitude (Table 1) as a result of the mechanical pretreatment. A clear increasing trend was observed in the conductivity of the PAN-derived carbon materials as a function of the mechanical pretreatment. The highest electrical conductivity registered for the PAN mats of fibers deposited by far-field electrospinning was on the order of 5,000 S/m. Our slightly higher values may stem from the fact that our 500  $\mu\text{m}$  thick samples were solid carbon sheets instead of the mats of



carbon fibers. It appears likely that despite the reported increase in the degree of graphitization from the previous study, the macroporosity of the interlaced PAN-derived carbon fibers may have limited the contribution of the increase in the degree of graphitization on the bulk electrical conductivity. Also, the dimensions of the mats of PAN fibers may have influenced the final conductivities obtained therein. In our case, since the conductivity did not vary when applying the mechanical compression pretreatment, we decided to investigate whether variations in the microstructure of the samples could be detected through Raman and XRD spectroscopy. It was hypothesized that variations in the microstructure of BPNE-derived carbon materials may be present in mechanically compressed samples as compared to the control even if the bulk electrical conductivity was not significantly altered by the mechanical pretreatment.

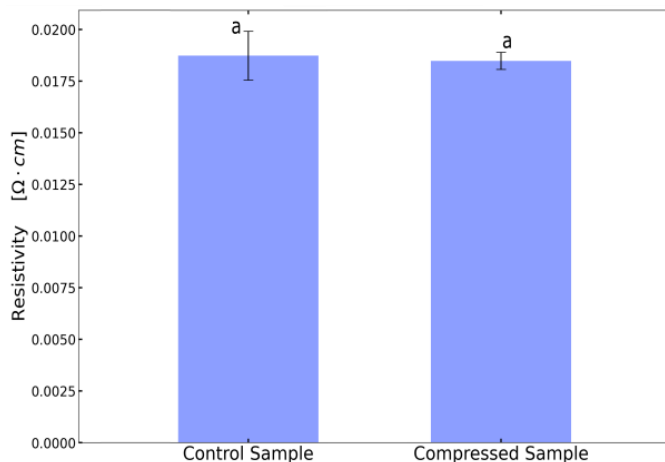


Figure 4. Bulk resistivity of carbon sheets derived from pyrolysis of Bis-phenol A Novolac Epoxy with and without the compressive pretreatment as obtained from the four-point-probe method ( $p > 0.05$  ANOVA) <sup>a</sup>.

We looked for variations in the Raman spectra of the pyrolyzed BPNE sheets, from which the microstructural tubostraticity of the crystallites is evaluated. Figure 5 shows the average of several Raman spectra collected for both groups of samples with and without the mechanical pretreatment along with the corresponding Lorentzian fittings. We analyzed the two characteristic peaks at  $\sim 1367$  and  $\sim 1600$   $\text{cm}^{-1}$  assigned to the D and  $E_{2g}$  bands, respectively. The 2D band was not analyzed in this study. The G ( $E_{2g}$ ) peak arises from the stretching motion of the  $\text{sp}^2$ -hybridized carbon-carbon bond in graphitic materials and the D peak corresponds to the degree of disorder around the graphitic microstructures present in the material. The intensity ratio of D peak to G peak and the breadth of the two bands are then commonly used as proxies for the relative degree of graphitization based on the crystallite size features  $L_a$  and  $L_c$ , related to the small in-lane correlation length and stack thickness. Hence, the higher the D to G ratio, the lower the alignment of graphenic planes is, thereby lowering the degree of graphitization in the carbon structure [25]. As it can be seen in Figure 5, the intensity of the peaks is the same for both groups of samples, yielding an  $I_D/I_G$  ratio of 1.02 (Table 1), coinciding with the graphite crystallite size and the degree of disorder obtained previously from the pyrolysis of phenol-formaldehyde and furan polymers, as well as for some bulk manufactured glass carbon materials (Table 1). The areas of both the D and G bands remain constant for both groups of samples, supporting the absence of an effect of the mechanical pretreatment. In comparison, compressive stress treatment of polyacrylonitrile with carbon nanotubes as templating agents yielded an  $I_D/I_G$  ratio of 0.69 [17], where a decreasing trend was observed from 1.26 to 0.69 as the material became more graphitic. In our case, we observe that the mechanical compression pretreatment does not appear to have a significant effect on the microstructure of the BPNE-derived carbon material in millimetric samples. This unexpected result may be related to the molecular structure of the Novolac epoxy resin, where the oxygen atoms within the network may be expected to cleave during pyrolysis into oxide radicals and byproducts. Cleavage at these sites could be expected to enhance the viscoelasticity and mobility of the percolated network during pyrolysis, precluding the effect of enhanced polymer crystallinity on the final carbon microstructure.

To corroborate the previous finding, in search for any evidence of microstructural variations, we looked into the 2D maps of the Raman analysis for topological nuances in the intensity of the D and G bands discussed above. As can be observed in Figure 5, the pyrolyzed BPNE-derived sheets with and without compression resulted in very similar 2D contour maps. We observed that in both cases the surface appears to be highly uniform. These results suggest that



there is an invariant degree of graphitization and microstructure at the surface of both groups of samples, and that the surface is smooth at least microscopically in the area analyzed on the surface of the pyrolyzed sheets. These observations agree with the results obtained for the resistivity, and appear to further indicate that indeed higher temperatures and mechanical loads may be required to induce a higher degree of alignment of the phenolic segments within the material before crosslinking to promote an increase in the degree of graphitization of the carbon material.

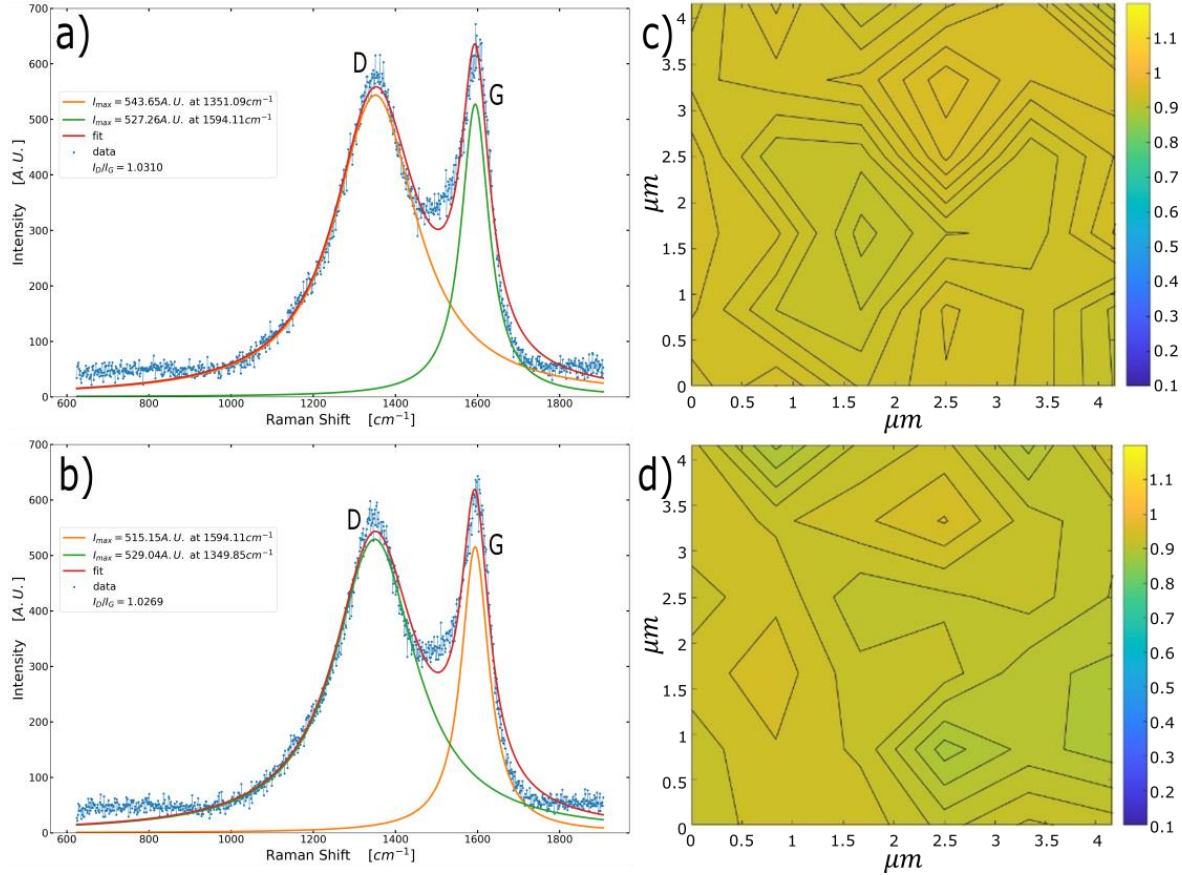


Figure 5. Raman spectrographs of pyrolyzed Bis-phenol A Novolac Epoxy sheets a) without and b) with compression before pyrolysis. 2D Raman analysis of the pyrolyzed films c) without compression and d) with compression.

In order to obtain a final confirmation for the lack of correlation between the compression pretreatment and the microstructure of BPNE-derived carbon material, we employed X-ray diffraction (XRD) spectroscopy to discern if there are any variations present between the two groups of samples, in terms of their relative degree of crystallinity. Two broad diffraction peaks can be observed in both groups of samples with and without compression of the uncured BPNE resin (Figure 6). The broad bands at  $22^\circ$  and  $55^\circ$  are related to the (002) plane and the (100) plane respectively [26]. The broadness of these peaks appears to be indicative of a low degree of stacking of the graphene crystallites in the (002) and (100) planes, for the interlayer spacing and crystallite size, as seen typically for non-graphitizing polymers. These spectra appear to agree with XRD spectra of similar glass-like carbon materials, where the mesoscale structure resembles that of semi-crystalline organic polymer networks. Most importantly, we observe no noticeable differences between the XRD spectra for the BPNE-derived sheets with and without the compression pretreatment. Thus, we can establish that this third evidence corroborates the lack of variations in the microstructure of the carbon material after applying the compression pretreatment to the uncured BPNE millimetric sheets at  $90^\circ \text{ C}$ . This result further supports the idea that any variation in the crystallinity of the uncured BPNE sheets that may have been caused by the mechanical compression pre-pyrolysis may result ineffectual to the properties of the BPNE-derived carbon. The latter may be due to the characteristic degree of mobility of BPNE-based samples during pyrolysis as evidenced by the shrinkage that is indicative a substantial amount of reconfiguration of the carbonizing crosslinked polymer.

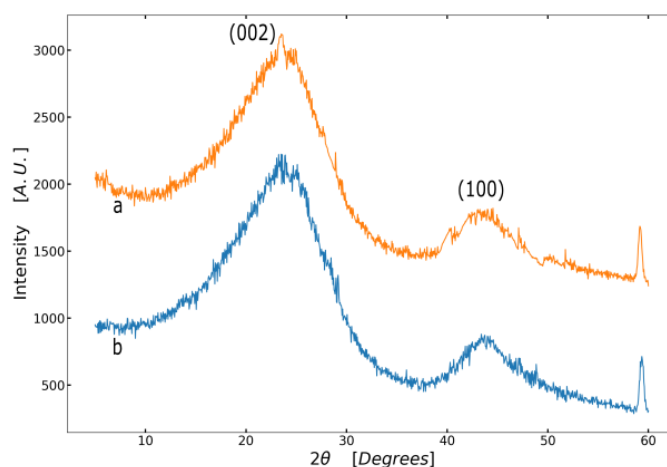


Figure 6. X-ray diffraction (XRD) patterns for millimetric sheets of carbon derived from BPNE a) without and b) with the compression pretreatment.

Although mechanical stresses were employed by others to successfully increase the degree of graphitization and electrical conductivity of carbon materials derived from macroscopic mats of PAN fibers [17], in this study, the microstructure and electrical properties of carbon materials derived from millimetric solid sheets of BPNE with and without the compression pretreatment remained the same. It is likely that some crosslinking may have been thermally induced during the compression pretreatment at 90°C through the thermal decomposition of the sulfonium salt. If polymer crosslinking were prematurely induced, the mobility of the material may be hampered so that the effect of mechanical compression on the crystallinity of the unpyrolyzed BPNE samples is reduced. However, we observe that the casted and uncured BPNE significantly deforms at the temperature used in this study during compression, which indicates that a minor degree of crosslinking occurred at this stage, if at all. The latter will have to be corroborated later by using FT-IR spectroscopy to monitor the degree of conversion of the epoxide groups throughout the process.

Furthermore, the absence of variations in the material from the application of the pretreatment may indicate that if the electrical conductivity of BPNE-derived carbon materials can be at all enhanced by mechanically altering the microstructure of the polymer, it would perhaps only occur at higher temperatures and compression loads. It has been stated that glass-like carbon is only formed from millimetric polymer samples at temperatures above 2000°C [27]. However, other reports mentioned that with appropriate heating rates, glass-like carbon may form at temperatures as low as 900-1000°C [25-28]. It appears that the matching of the heating rate and the intermediate dwelling temperature to the sample dimensions and polymer structure is key to allow the flow of the material and the reorganization of its microstructure during the pre-carbonization stage. The latter has been proposed to be crucial for the formation of the turbostratic features and the percolated graphenic, or fullerenic, percolated network characteristic of glass-like carbon. It is important to note that the internal stresses per unit volume that drive the viscoelastic deformation of the material during carbonization can certainly be expected to be greater than the ones reached in the compression pretreatment. Therefore, our hypothesis may be further tested through subsequent experiments on smaller sample geometries to confirm that size-dependent factors were not influencing the results obtained in this initial proof-of-concept study.

Interestingly, the viscoelastic behavior of BPNE samples during carbonization has been linked to the heteroatoms present in the polymer structure, which are degassed from the final carbon material during the carbonization stage (300-1200 °C) [29]. It has been stipulated that heteroatoms are completely degassed at higher temperatures, 1200-2000 °C, than the one used here, 900°C. However, Cardenas-Benitez et al. reported a considerable reduction in the oxygen atom content in BPNE-derived suspended carbon nanowires from 62 % to 8 % after pyrolysis by energy dispersive X-ray spectroscopy [12]. The latter agrees well with the expected 90 % carbon content in the pyrolytic residue from crosslinked photopolymers carbonized up to 900 °C [29]. Others have assumed that the oxygen atoms are completely removed pyrolyzed to around 1000°C in BPNE samples [28]. In the end, it can be expected that most of the oxygen content may be lost in the samples used for this study, albeit perhaps less than for the microwires, considering the size and geometrical differences. Most importantly, the oxygen loss in during pyrolysis of BPNE implies that a substantial number of the crosslinks formed during photopolymerization may be lost as a result of

thermal cleavage of the ether bonds linked to the epoxides that serve as crosslinking functional groups; recalling that the initial oligomer is likely an octamer. As the temperature increases inside the BPNE samples, sufficient energy is provided to break the C-O bonds that bridge between the bisphenolic core and the  $n=8$  functional groups. As this occurs, the degree of crosslinking of the polymer network will change. It is unknown how many original crosslinks are replaced by C-C bonds from radical-radical recombination during the carbonization stage. If the polymer becomes temporarily more loosely crosslinked, its viscoelasticity increases. If the rates of change of the mechanical properties of the material matches the rate of byproduct degassing, a substantial amount of movement and reconfiguration of the remaining crosslinked carbon network may occur. The latter must be tightly linked to the significant thermally induced deformation and flow of BPNE samples as compared to that of other polymers, such as crosslinked PAN, with fewer C-O bonds. The latter may be expected to preclude the alteration of the microstructure of the carbon material via the pre-pyrolysis perturbation of the polymer microstructure; for the most substantial reorganization of the microstructure of the material will occur during pyrolysis. The latter may point to the fact that this molecular structural feature may be crucial to understand how BPNE yields carbon structures with such a unique set of properties, which have made it so useful for the production of glass-like carbon. Furthermore, this observation points to the need to analyze the polymer degradation dynamics and mechanism during pyrolysis in order to better understand the role of C-O cleavage.

The hypothesis that the ether linkages in the pyrolysis of BPNE appears to have a crucial role in glass-like carbon formation agree well with the documented links between the heating rate and the intermediate dwelling temperature, and glass-like carbon synthesis [27]. For instance, an intermediate dwelling temperature of 300°C has been extensively used for the pyrolysis of BPNE samples of multiple ranges of sizes and geometries [22, 23, 27]. The selection of this particular temperature may be related to the known  $T_g$  values for crosslinked BPNE of around 200-300 °C, depending on the crosslink density. It has been previously proposed that heating polymers to a temperature just above their  $T_g$  allows a percolated carbon network to form by allowing the “annealing” of gas pockets and the appropriate crystallite growth [27]. On the other hand, typical heating rates for BPNE samples in the micro and macro scales have been reported to be around 2-5 °C/min [22-28]. Pramanick et al. investigated the effect of the heating rate on the atomic composition and microstructure of BPNE-derived carbon materials. Heating rates between 2 and 20 °C/min were analyzed. They documented a somewhat unexpected trend where the C:O ratio in the pyrolyzed carbon goes through a maximum at about 5 °C/min and decreases slightly and seemingly randomly as the heating rate increases. The latter appears to be indicative of a complex relation between heating rate and the carbon microstructure. If the heating and polymer degradation rates do not allow for an appropriate degassing rate to match the viscoelastic deformation rate of the material, it may result in sample fracture or otherwise lead to drastically different microstructural features. In the present study, we utilized a substantially higher heating rate of 30°C/min. It is entirely surprising that glass-like carbon was formed at this higher heating rate and with a longer dwelling time of 3 hours at 300°C, based on sample size. It is possible that this adjusted heat-treatment protocol may have led to the successful synthesis of glass-like carbon even in the relatively large millimetric solid sheets of BPNE used in the present study. From these observations, a reasonable next step can be to investigate the effect of the degree of crosslinking of BPNE on the behavior of the material during pyrolysis at a carefully chosen heating rates and intermediate temperatures selected as a function of the  $T_g$  of the initial crosslinked polymer, which can be varied by changing the UV exposure time to control the polymer crosslink density.

#### 4. Conclusion

In this study, we tested the hypothesis that the structure and the resistivity of carbon materials derived from the pyrolysis of millimeter-scale sheets of Bis-phenol A Novolac Epoxy can be increased by a mechanical compression pretreatment pre-pyrolysis. First, the values obtained for the resistivity of the carbon samples indicated the absence of noticeable variations in the macroscopic electrical behavior between the materials synthesized with and without the compression pretreatment. Then, Raman spectroscopy and XRD supported the finding that there does not seem to be any significant variations in the graphitic crystallite size and the degree of microstructural order between the samples with and without a compression pretreatment reaching a compressive stress of up to 50 MPa. We cannot conclude from this study if the electrical properties of BPNE-derived carbon materials can be at all enhanced by modifying the fabrication protocol with the addition mechanical or other types of pretreatments. However, from this initial study we showed that it seems unfeasible to achieve the latter goal with the fabrication process used herein. Therefore, it appears that if mechanical deformation resulting from the internal stresses develop during pyrolysis of the phenolic epoxide precursors takes part in the previously documented increase in electrical conductivity, the stresses therein must be considerable higher than the ones used here. Furthermore, it is proposed that the present result may be also explained

if the most crucial factor influencing the microstructure of BPNE-derived carbon is the loss temperature-dependent decrease in crosslink density, which may result in a unique viscoelastic behavior during carbonization. If so, any alignment of the phenolic cores and any degree of order induced in the polymer sample via  $\pi$ - $\pi$  stacking may be ineffectual as the material will undergo a substantial amount of reconfiguration during volume loss. This study serves as starting point in the search of relatively low-cost methods to obtain glass-like carbon materials with a slightly more graphitic character derived from organic polymer precursors that can be easily patterned into functional geometries.

## Acknowledgements

Authors would like to thank the financial support from Tecnológico de Monterrey as part of the China-Tec Research Initiative for the development of photosensitive materials. O.K.T. thanks financial support from CONACYT (grant no. 2019-000002-01NACF). We thank Prof. Dr. Marcelo Videa and Dr. Sunny Holmberg for access to the XRD and the Raman spectrophotometers, respectively. A special acknowledgment to the Centro del Agua at Tecnológico de Monterrey for access to the Raman facility. We thank Dr. Arnoldo Sanchez for guidance with the four-point-probe method. We also thank financial support from the Nanosensors and Devices Research Group at Tecnológico de Monterrey (0020209I06). A.A.S thanks the Department for Sustainable Technologies and Civil Engineering for additional support.

## Nomenclature

BPNE	Bis-phenol A Novolac Epoxy
PDMS	Poly-dimethylsiloxane
PAN	Poly-acrylonitrile
MEMS	Microelectromechanical systems
XRD	X-ray diffraction
UV	Ultraviolet

## References

- [1] R.L. McCreery, Advanced Carbon Electrode Materials for Molecular Electrochemistry, *Chem. Rev.* 108 (2008) 2646–2687.
- [2] A.K. Geim, Random Walk to Graphene (Nobel Lecture), *Angew. Chemie Int. Ed.* 50 (2011) 6966–6985.
- [3] M.J. Allen, V.C. Tung, R.B. Kaner, Honeycomb Carbon: A Review of Graphene, *Chem. Rev.* 110 (2010) 132–145.
- [4] Y. Zhu, S. Murali, W. Cai, X. Li, J.W. Suk, J.R. Potts, R.S. Ruoff, Graphene and Graphene Oxide: Synthesis, Properties, and Applications, *Adv. Mater.* 22 (2010) 3906–3924.
- [5] M. Katsnelson, A. Geim, Electron scattering on microscopic corrugations in graphene, *Philos. Trans. R. Soc. A Math. Phys. Eng. Sci.* 366 (2008) 195–204.
- [6] D. Li, R.B. Kaner, MATERIALS SCIENCE: Graphene-Based Materials, *Science*. 320 (2008) 1170–1171.
- [7] A.K. Geim, K.S. Novoselov, The rise of graphene, *Nat. Mater.* 6 (2007) 183–191.
- [8] A.K. Geim, Graphene: Status and Prospects, *Science*. 324 (2009) 1530–1534.
- [9] H.C. Schniepp, J.-L. Li, M.J. McAllister, H. Sai, M. Herrera-Alonso, D.H. Adamson, R.K. Prud'homme, R. Car, D.A. Saville, I.A. Aksay, Functionalized Single Graphene Sheets Derived from Splitting Graphite Oxide, *J. Phys. Chem. B*. 110 (2006) 8535–8539.
- [10] H.C. Schniepp, K.N. Kudin, J.-L. Li, R.K. Prud'homme, R. Car, D.A. Saville, I.A. Aksay, Bending Properties of Single Functionalized Graphene Sheets Probed by Atomic Force Microscopy, *ACS Nano*. 2 (2008) 2577–2584.
- [11] M.F. El-Kady, V. Strong, S. Dubin, R.B. Kaner, Laser Scribing of High-Performance and Flexible Graphene-Based Electrochemical Capacitors, *Science*. 335 (2012) 1326–1330.
- [12] B. Cardenas-Benitez, C. Eschenbaum, D. Mager, J.G. Korvink, M.J. Madou, U. Lemmer, I. De Leon, S.O. Martinez-Chapa, Pyrolysis-induced shrinking of three-dimensional structures fabricated by two-photon polymerization: experiment and theoretical model, *Microsystems Nanoeng.* 5 (2019) 38.
- [13] B.Y. Park, L. Taherabadi, C. Wang, J. Zoval, M.J. Madou, Electrical Properties and Shrinkage of Carbonized Photoresist Films and the Implications for Carbon Microelectromechanical Systems Devices in

- Conductive Media, *J. Electrochem. Soc.* 152 (2005) J136.
- [14] G. Canton, T. Do, L. Kulinsky, M. Madou, Improved conductivity of suspended carbon fibers through integration of C-MEMS and Electro-Mechanical Spinning technologies, *Carbon N. Y.* 71 (2014) 338–342.
  - [15] N. Liu, K. Kim, H.Y. Jeong, P.C. Hsu, Y. Cui, Z. Bao, Effect of Chemical Structure on Polymer-Templated Growth of Graphitic Nanoribbons, *ACS Nano.* 9 (2015) 9043–9049.
  - [16] A. Allaoui, S.V. Hoa, M.D. Pugh, The electronic transport properties and microstructure of carbon nanofiber/epoxy composites, *Compos. Sci. Technol.* 68 (2008) 410–416.
  - [17] M. Ghazinejad, S. Holmberg, O. Pilloni, L. Oropeza-Ramos, M. Madou, Graphitizing Non-graphitizable Carbons by Stress-induced Routes, *Sci. Rep.* 7 (2017) 16551.
  - [18] T. Maitra, S. Sharma, A. Srivastava, Y.K. Cho, M. Madou, A. Sharma, Improved graphitization and electrical conductivity of suspended carbon nanofibers derived from carbon nanotube/polyacrylonitrile composites by directed electrospinning, *Carbon N. Y.* 50 (2012) 1753–1761.
  - [19] D. Mattia, M.P. Rossi, B.M. Kim, G. Korneva, H.H. Bau, Y. Gogotsi, Effect of Graphitization on the Wettability and Electrical Conductivity of CVD-Carbon Nanotubes and Films, *J. Phys. Chem. B.* 110 (2006) 9850–9855.
  - [20] S. Holmberg, M. Ghazinejad, E. Cho, D. George, B. Pollack, A. Perebikovskiy, R. Ragan, M. Madou, Stress-activated pyrolytic carbon nanofibers for electrochemical platforms, *Electrochim. Acta.* 290 (2018) 639–648.
  - [21] M. Yoonessi, J.R. Gaier, M. Sahimi, T.L. Daulton, R.B. Kaner, M.A. Meador, Fabrication of Graphene–Polyimide Nanocomposites with Superior Electrical Conductivity, *ACS Appl. Mater. Interfaces.* 9 (2017) 43230–43238.
  - [22] B. Xue, Y. Zou, Y. Yang, A photochemical approach for preparing graphene and fabrication of SU-8/graphene composite conductive micropatterns, *Mater. Des.* 132 (2017) 505–511.
  - [23] B. Pramanick, M. Vazquez-Pinon, A. Torres-Castro, S.O. Martinez-Chapaa, M. Madou, Effect of pyrolysis process parameters on electrical, physical, chemical and electro-chemical properties of SU-8-derived carbon structures fabricated using the C-MEMS process, *Mater. Today Proc.* 5 (2018) 9669–9682.
  - [24] J.-Y. Lee, J.-M. Jung, D.-Y. Kim, Y.S. Lee, C.-H. Jung, K. Shin, J.-H. Choi, Preparation of Conductive Carbon Films from Poly(vinyl alcohol) by Chemical Pre-Treatment and Pyrolysis, *J. Nanosci. Nanotechnol.* 17 (2017) 5481–5484.
  - [25] Y.M. Hassan, C. Caviglia, S. Hemanth, D.M.A. Mackenzie, T.S. Alstrøm, D.H. Petersen, S.S. Keller, High temperature SU-8 pyrolysis for fabrication of carbon electrodes, *J. Anal. Appl. Pyrolysis.* 125 (2017) 91–99.
  - [26] S. Mamidi, M. Kakunuri, C.S. Sharma, Fabrication of SU-8 Derived Three-Dimensional Carbon Microelectrodes as High Capacity Anodes for Lithium-Ion Batteries, *ECS Trans.* 85 (2018) 21–27.
  - [27] S. Sharma, Glassy Carbon: A Promising Material for Micro- and Nanomanufacturing, *Materials (Basel).* 11 (2018) 1857.
  - [28] A. Salazar, S. Hosseini, M. Sanchez-Domínguez, M.J. Madou, A. Montesinos-Castellanos, S.O. Martinez-Chapa, Sub-10 nm nanogap fabrication on suspended glassy carbon nanofibers, *Microsystems Nanoeng.* 6 (2020) 9.
  - [29] R. Martinez-Duarte, SU-8 Photolithography as a Toolbox for Carbon MEMS, *Micromachines.* 5 (2014) 766–782.